

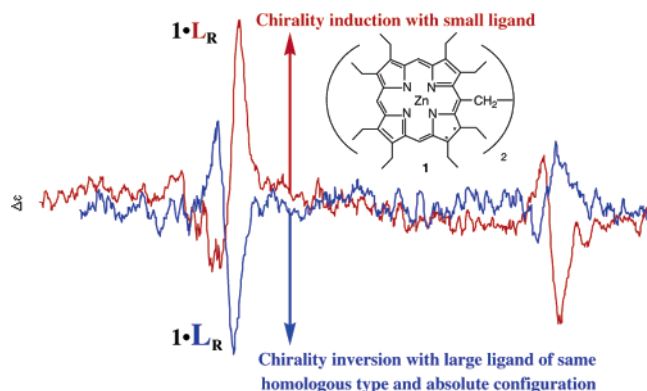
Supramolecular Chirogenesis with Bis-chlorin versus Bis-porphyrin Hosts: Peculiarities of Chirality Induction and Modulation of Optical Activity

Victor V. Borovkov,* Guy A. Hembury, and Yoshihisa Inoue*

Entropy Control Project, ICORP, JST, 4-6-3 Kamishinden, Toyonaka-shi, Osaka 560-0085, Japan

victrb@inoue.jst.go.jp; inoue@chem.eng.osaka-u.ac.jp

Received May 27, 2005



The complexation behavior, chirality induction and inversion in the achiral host, a racemic mixture of ethane-bridged bis(zinc octaethylchlorin) (**1**), and optical activity modulation in the chiral hosts, enantiopure **1_R** and **1_S**, upon interaction with chiral and achiral amine guests have been investigated by means of the UV–vis, CD, and ¹H NMR techniques and compared with the corresponding spectral data of the bis-porphyrin analogue. It was found that the chirogenesis pathway is strongly dependent upon the structures of both major components (hosts and guests) of these supramolecular systems. Particularly, the distinct orientation of electronic transitions in the chlorin chromophores arisen from the reduced pyrrole ring, which makes it radically different from that of the porphyrin chromophores, and the size of the guest's substituents lead to the remarkable phenomenon of chirality induction-inversion in racemic **1** originating from the process of asymmetry transfer from enantiopure guests of the same homologous type and absolute configuration. This surprising chirogenic behavior is found to be in a sharp contrast to that observed in the analogous porphyrin-based systems. Furthermore, these structural and electronic phenomena also account for the effective optical activity quenching of enantiopure **1_R** and **1_S** upon interaction with chiral and with achiral amines, which results in formation of supramolecular complexes of opposite chirality.

Introduction

In recent years considerable progress in the field of supramolecular chemistry and its combination with new insights into molecular chirality has given rise to a new interdisciplinary area of chemistry—supramolecular chirality—whose rapid growth derives from its direct relevance to many natural processes and artificial systems, as well as its importance for understanding fundamental chemical principles and vital biological functions and its applicability in various chiroptical devices and modern molecular technologies.¹ This area includes the processes of immediate asymmetry transfer from a

chiral guest to an achiral host (or vice versa) via noncovalent interactions, chirality induction in achiral supramolecular complexes affected by the external chiral field and environment, chirality amplification of whole assemblies upon association of the individual elements with a low degree of asymmetry, and spontaneous resolution of racemic supramolecular systems. Comprehensive investigation of the corresponding driving forces, detailed mechanisms, and controlling factors is a crucial requirement for the understanding and effective implementation of the phenomenon of supramolecular chirogenesis. One of the most important prerequisites to the success of such studies lies in the fact that the monitoring parameters

(such as the electronic transitions, chemical shifts, etc.) should be in a spectral region isolated from and not overlapping with the rest of the parameters belonging to other components of the supramolecular system. In this light, porphyrin molecules were found to be exceptionally suitable chromophores for following chirogenic processes occurring in host–guest assemblies owing to their unique spectral and physicochemical properties, as well as easy handling, versatile synthetic modifications, great biological importance, and wide applicability. Particularly, dimeric and oligomeric porphyrin structures are found to be of special interest because of their high sensitivity toward through-space interporphyrin electronic communication, even over relatively large distances.^{1a–g,j,k,m,u,v,2} This allows effective detection and facile monitoring of the asymmetry information transfer arising from stereospecific arrangements of the chromophoric units induced by an external chiral field, and prompted us and other research groups to widely employ these types of porphyrin systems for studying the supramolecular chirogenesis phenomenon.

Our previous supramolecular chirogenic systems were mainly based upon achiral bis-porphyrin hosts (various metallo-complexes of bis-octaethylporphyrin) in which two porphyrin subunits are connected by an ethane bridge (see **1_{Por}** in Figure 1), and different chiral guests.^{1a,3} This covalent linker of **1_{Por}** plays a decisive and dual role in the process of asymmetry transfer. The first and most important function is that the two chromophores are kept in close proximity to each other, thus allowing effective through-space electronic communication, which is a key factor for any chirogenic phenomenon. In the case of **1_{Por}** this function's importance is further enhanced by extremely strong interporphyrin interactions in nonpolar solvents, resulting in a syn (face-to-face) spatial arrange-

ment of the two porphyrins in the original **1_{Por}**, which can be easily destroyed upon complexation with external ligands to yield an extended anti (in-line) conformation.^{1a,2g,3b–e,g–m} Additionally, this switching effect offers a great advantage in the monitoring process of supramolecular chirogenesis because of the considerable differences in spectral properties of these two rotational conformers. The second important factor is the linkage's semi-flexibility/semi-rigidity provided by the relatively short but flexible C₂ chain. This makes it possible for **1_{Por}** to effectively sense the chiral environment (even in the case of a rather low degree of asymmetry) by adopting the corresponding stereospecific conformation, which is stable enough to be easily detected by conventional circular dichroism (CD) spectroscopy. For example, the two porphyrin units in **1_{Por}** can freely rotate around the C–C bond of the ethane bridge, thus enabling the syn–anti conformational switching and further chiral deformations, but crucially, it cannot flip over around the bonds between the ethane bridge and the porphyrin's meso carbons, hence preventing the racemization process. In this manner these particular properties ensure high efficiency of the supramolecular chirogenesis in **1_{Por}**.

The specific mechanism of chirality induction in **1_{Por}** includes competitive repulsive interactions between the two bulkiest substituents at the ligand's stereogenic center and the ethyl groups of the neighboring porphyrin ring at the *a*- or *b*-positions (see Figure 1) upon “inside coordination” of the chiral ligand (inside binding occurs from the side of the porphyrin that results in a close spatial proximity between the ligand and the adjacent ethyl groups).⁴ Under these conditions, it is clear that the substituents' relative sizes are one of the major elements which determine the strength and magnitude of these steric repulsions. Hence, it is the bulkiest group, in particular, that was found to interact most strongly

(1) Selected examples of supramolecular chirality in various systems: (a) Borovkov, V. V.; Hembury, G. A.; Inoue, Y. *Acc. Chem. Res.* **2004**, *37*, 449. (b) Yamaguchi, T.; Kimura, T.; Matsuda, H.; Aida, T. *Angew. Chem., Int. Ed.* **2004**, *43*, 6350. (c) Hwang, I.-W.; Kamada, T.; Ahn, T. K.; Ko, D. M.; Nakamura, T.; Tsuda, A.; Osuka, A.; Kim, D. *J. Am. Chem. Soc.* **2004**, *126*, 16187. (d) Guo, Y.-M.; Oike, H.; Aida, T. *J. Am. Chem. Soc.* **2004**, *126*, 716. (e) Balaban, T. S.; Bhise, A. D.; Fischer, M.; Linke-Schaetzl, M.; Roussel, C.; Vanthuyne, N. *Angew. Chem., Int. Ed.* **2003**, *42*, 2140. (f) Borovkov, V. V.; Harada, T.; Hembury, G. A.; Inoue, Y.; Kuroda, R. *Angew. Chem., Int. Ed.* **2003**, *42*, 1746. (g) Pescitelli, G.; Gabriel, S.; Wang, Y.; Fleischhauer, J.; Woody, R. W.; Berova, N. *J. Am. Chem. Soc.* **2003**, *125*, 7613. (h) Nabeshima, T.; Hashiguchi, A.; Saiki, T.; Akine, S. *Angew. Chem., Int. Ed.* **2002**, *41*, 481. (i) Ishikawa, M.; Maeda, K.; Yashima, E. *J. Am. Chem. Soc.* **2002**, *124*, 7448. (j) Tsukube, H.; Shinoda, S. *Chem. Rev.* **2002**, *102*, 2389. (k) Ribó, M.; Crusats, J.; Sagüés, F.; Claret, J.; Rubires, R. *Science* **2001**, *292*, 2063. (l) de Loos, M.; van Esch, J.; Kellogg, R. M.; Feringa, B. L. *Angew. Chem., Int. Ed.* **2001**, *40*, 613. (m) Jung, J. H.; Kobayashi, H.; Masuda, M.; Shimizu, T.; Shinkai, S. *J. Am. Chem. Soc.* **2001**, *123*, 8785. (n) Brunsveld, L.; Meijer, E. W.; Prince, R. B.; Moore, J. S. *J. Am. Chem. Soc.* **2001**, *123*, 7978. (o) Nakashima, H.; Koe, J. R.; Torimitsu, K.; Fujiki, M. *J. Am. Chem. Soc.* **2001**, *123*, 4847. (p) Iarossi, D.; Mucci, A.; Parenti, F.; Schenetti, L.; Seeber, R.; Zanardi, C.; Forni, A.; Tonelli, M. *Chem. Eur. J.* **2001**, *7*, 676. (q) Steffen, W.; Kohler, B.; Altmann, M.; Scherf, U.; Stitzer, K.; zur Loye, H.-C.; Bunz, U. H. F. *Chem. Eur. J.* **2001**, *7*, 117. (r) Zahn, S.; Proni, G.; Spada, G. P.; Canary, J. W. *Chem. Eur. J.* **2001**, *7*, 88. (s) Rivera, J. M.; Martin, T.; Rebek, J., Jr. *Science* **2000**, *289*, 606. (t) Wang, M.; Silva, G. L.; Armitage, B. A. *J. Am. Chem. Soc.* **2000**, *122*, 9977. (u) Purrello, R.; Raudino, A.; Scolaro, L. M.; Loisi, A.; Bellacchio, E.; Lauceri, R. *J. Phys. Chem. B* **2000**, *104*, 10900. (v) Steensgaard, D. B.; Wackerbarth, H.; Hildebrandt, P.; Holzwarth, A. R. *J. Phys. Chem. B* **2000**, *104*, 10379. (w) Fox, J. M.; Katz, T. J.; Van Elshocht, S.; Verbiest, T.; Kauranen, M.; Persoons, A.; Thongpanchang, T.; Kraus, T.; Brus, L. *J. Am. Chem. Soc.* **1999**, *121*, 3453. (x) Ogoshi, H.; Mizutani, T. *Acc. Chem. Res.* **1998**, *31*, 81. (y) Wittung, P.; Nielsen, P.; Buchart, O.; Egholm, M.; Norden, B. *Nature* **1994**, *368*, 561.

(2) The selected examples of various chiral and achiral bis- and multiporphyrin systems: (a) Choi, M.-S.; Yamazaki, T.; Yamazaki, I.; Aida, T. *Angew. Chem., Int. Ed.* **2004**, *43*, 150. (b) Balaban, T. S.; Goddard, R.; Linke-Schaetzl, M.; Lehn, J.-M. *J. Am. Chem. Soc.* **2003**, *125*, 4233. (c) Okada, S.; Segawa, H. *J. Am. Chem. Soc.* **2003**, *125*, 2792. (d) Takahashi, R.; Kobuke, Y. *J. Am. Chem. Soc.* **2003**, *125*, 2372. (e) Kubo, Y.; Ohno, T.; Yamanaka, J.-i.; Tokita, S.; Iida, T.; Ishimaru, Y. *J. Am. Chem. Soc.* **2001**, *123*, 12700. (f) Brettar, J.; Gisselbrecht, J.-P.; Gross, M.; Solladié, N. *Chem. Commun.* **2001**, 733. (g) Borovkov, V. V.; Lintuluoto, J. M.; Inoue, Y. *J. Phys. Chem. B* **1999**, *103*, 5151. (h) Borovkov, V. V.; Lintuluoto, J. M.; Inoue, Y. *Helv. Chim. Acta* **1999**, *82*, 919. (i) Sessler, J. L.; Andrievsky, A.; Kral, V.; Lynch, V. *J. Am. Chem. Soc.* **1997**, *119*, 9385. (j) Hayashi, T.; Nonoguchi, M.; Aya, T.; Ogoshi, H. *Tetrahedron Lett.* **1997**, *38*, 1603. (k) Ema, T.; Misawa, S.; Nemugaki, S.; Sakai, T.; Utaka, M. *Chem. Lett.* **1997**, 487. (l) Crossley, M. J.; Mackay, L. G.; Try, A. C. *J. Chem. Soc., Chem. Commun.* **1995**, 1925. (m) Wasielewski, M. R. *Chem. Rev.* **1992**, *92*, 435.

(3) (a) Borovkov, V. V.; Fujii, I.; Muranaka, A.; Hembury, G. A.; Tanaka, T.; Ceulemans, A.; Kobayashi, N.; Inoue, Y. *Angew. Chem., Int. Ed.* **2004**, *43*, 5481. (b) Borovkov, V. V.; Hembury, G. A.; Inoue, Y. *Angew. Chem., Int. Ed.* **2003**, *42*, 5310. (c) Borovkov, V. V.; Lintuluoto, J. M.; Hembury, G. A.; Sugiura, M.; Arakawa, R.; Inoue, Y. *J. Org. Chem.* **2003**, *68*, 7176. (d) Borovkov, V. V.; Hembury, G. A.; Yamamoto, N.; Inoue, Y. *J. Phys. Chem. A* **2003**, *107*, 8677. (e) Borovkov, V. V.; Harada, T.; Inoue, Y.; Kuroda, R. *Angew. Chem., Int. Ed.* **2002**, *41*, 1378. (f) Borovkov, V. V.; Lintuluoto, J. M.; Sugiura, M.; Inoue, Y.; Kuroda, R. *J. Am. Chem. Soc.* **2002**, *124*, 11282. (g) Borovkov, V. V.; Lintuluoto, J. M.; Inoue, Y. *Org. Lett.* **2002**, *4*, 169. (h) Borovkov, V. V.; Lintuluoto, J. M.; Sugeta, H.; Fujiki, M.; Arakawa, R.; Inoue, Y. *J. Am. Chem. Soc.* **2002**, *124*, 2993. (i) Borovkov, V. V.; Lintuluoto, J. M.; Inoue, Y. *J. Am. Chem. Soc.* **2001**, *123*, 2979. (j) Borovkov, V. V.; Yamamoto, N.; Lintuluoto, J. M.; Tanaka, T.; Inoue, Y. *Chirality* **2001**, *13*, 329. (k) Borovkov, V. V.; Lintuluoto, J. M.; Fujiki, M.; Inoue, Y. *J. Am. Chem. Soc.* **2000**, *122*, 4403. (l) Borovkov, V. V.; Lintuluoto, J. M.; Inoue, Y. *Org. Lett.* **2000**, *2*, 1565. (m) Borovkov, V. V.; Lintuluoto, J. M.; Inoue, Y. *J. Phys. Chem. A* **2000**, *104*, 9213.

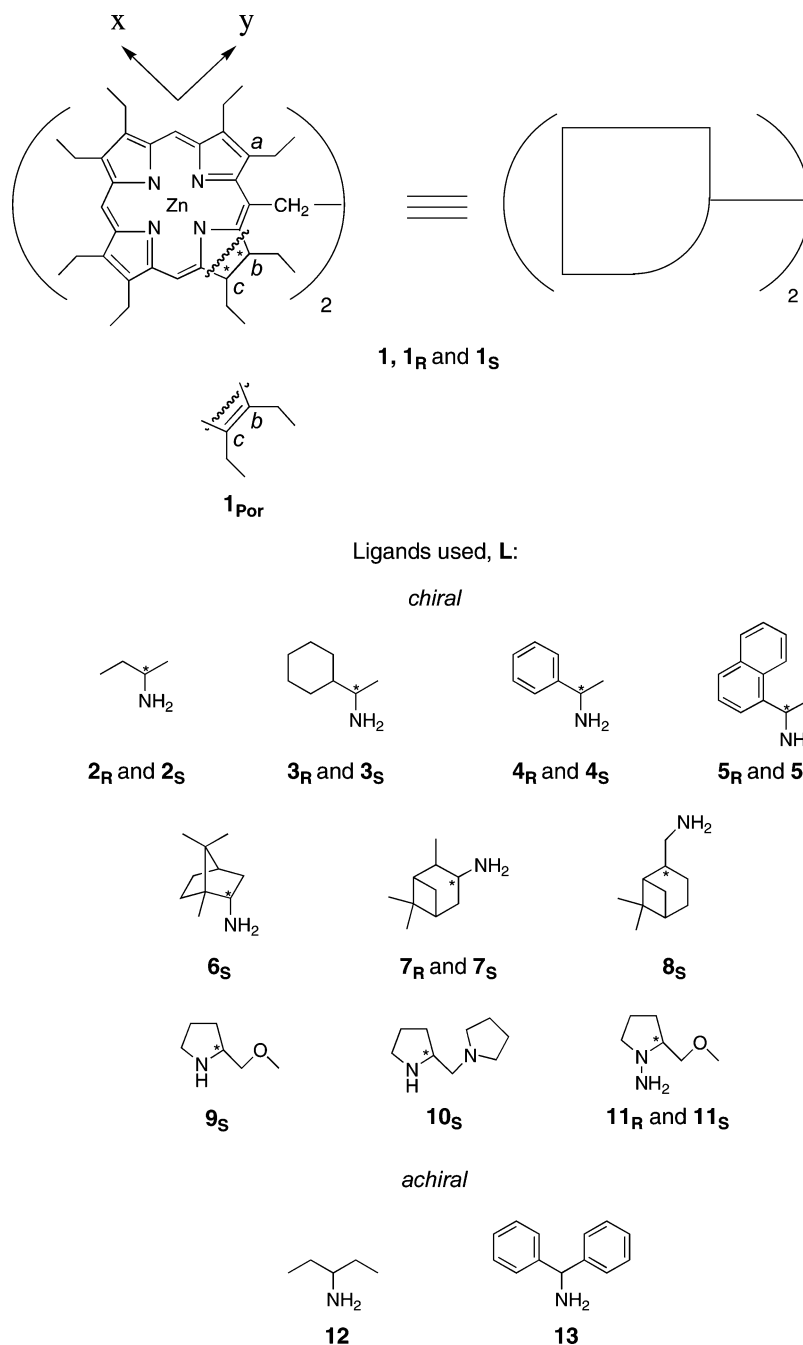


FIGURE 1. Structures of bis-chromophore hosts (bis-chlorins: achiral **1** and chiral **1_R/1_S** and bis-porphyrin **1_{Por}**) and amine guests (**L**: chiral **2–11** and achiral **12** and **13**). The subscript (**R** or **S**) indicates the absolute configuration of the asymmetric carbon, which is marked by asterisk.

with one of the corresponding ethyl groups, thus forcing the neighboring porphyrin ring to move outward and inducing the unidirectional twist in **1_{Por}** that results in translating the guest's asymmetry into the host's chirality. In the case of conventional monodentate ligands of which the substituent size order at the stereogenic center

correlates with the Cahn–Ingold–Prelog priority rule system for absolute configuration assignment, it was found that ligated (*S*)-enantiomers having the bulkiest group on the left position (upon viewing from the side opposite to the binding group) produce a right-handed screw structure, while for (*R*)-enantiomers the situation is a simple mirror image. As this takes place, the corresponding porphyrin electronic transitions are coupled in a stereospecific fashion producing a moderate-to-strong CD signal in the region of the porphyrin high-energy Soret (B) band consisting of two major Cotton effects, the sign of which depends on the induced helicity in **1_{Por}**. For example, the right-handed screw generates positive

(4) The “inside coordination” implies that a ligand approaches from the side of the neighboring chlorin moiety (and is, thus, close spatial proximity to it), while the “outside coordination” implies that a ligand approaches from the side opposite to the neighboring chlorin moiety (and is, thus, spatially distant from it). It was previously shown that only inside coordination for bis-porphyrins, and their subsequent chiral steric interactions, are responsible for supramolecular chirogenesis in these systems (for details see ref 3d).

chirality, while the opposite handedness yields a correspondingly negative sign. This regularity allows $\mathbf{1}_{\text{Por}}$ to be effectively used as a highly sensitive chirality sensor for the assignment of absolute configuration of external guests.

However, application of the porphyrin chromophores for investigation of the phenomenon of supramolecular chirogenesis is limited by the narrow spectral region of the most intense B band (about 350–450 nm), where some chiral guests may also absorb the light, thus hampering the monitoring process. In relation to this shortcoming, other types of bathochromically shifted pigments are of special interest. Of particular potential are the related chlorin structures possessing a reduced pyrrole ring, which causes, besides an intense B absorption, a pronounced enhancement of the lowest singlet-energy transition (Q) band in the visible spectral region. This remarkable advantage is effectively utilized by nature to ensure high efficiency in the process of photosynthesis,⁵ and is successfully used in a large variety of biomimetic systems.⁶ However, to date, this attractive property has not been applied to the investigation of supramolecular chirogenesis. To overcome this gap and considerably expand the diversity of this chromophoric system's potential suitability for chirality sensing purposes, we have undertaken, for the first time, to study this new host–guest system on the basis of racemic and enantiopure ethane-bridged bis(zinc octaethylchlorin)s (see $\mathbf{1}$ and $\mathbf{1}_R/\mathbf{1}_S$ in Figure 1)^{7–9} upon interaction with various chiral and achiral amine ligands.

Results and Discussion

1. Supramolecular Systems. The prime reason for the choice of bis-chlorins (racemic $\mathbf{1}$ and enantiopure $\mathbf{1}_R$ and $\mathbf{1}_S$),^{7–9} which are connected by a short covalent bridge, as suitable host molecules for the study of supramolecular chirogenic processes was based on their chemical resemblance to the bis-porphyrin host $\mathbf{1}_{\text{Por}}$ (Figure 1), which to date has been well-studied and effectively used as a chirality sensor.^{1a,3} However, it is important to note that there are several crucial distinctions between the chlorin and porphyrin hosts caused by the reduced pyrrole ring of the chlorin macrocycle that should be taken into account upon analyzing the results of the host–guest associations. First is a noticeable difference in the initial spatial geometries of these hosts

in their non-interacting forms. In the case of $\mathbf{1}_{\text{Por}}$ both porphyrin subunits are closely overlapped in a parallel orientation owing to the compact folded syn conformation as mentioned above (see Introduction section) and the well-known planarity of zinc porphyrin complexes.¹⁰ However $\mathbf{1}$, in contrast to $\mathbf{1}_{\text{Por}}$, exists in a more opened and twisted conformation, apparently due to the steric hindrances imposed by the four sp^3 carbons, in which two chlorin macrocycles are spaced farther apart from each other with its reduced pyrrole rings overlapped loosely along *b*-positions.^{9,11} This geometry resembles that of the corresponding tweezer structure generated in $\mathbf{1}_{\text{Por}}$ upon interaction with bidentate ligands.^{1a,3a,c,f,g} These geometrical differences are expected to influence the degree of spectral changes caused by interaction with external guests as will be demonstrated below. The second important point is the different polarizations of the electronic transitions in $\mathbf{1}_{\text{Por}}$ and $\mathbf{1}$, which are dictated by the chromophoric structure and molecular symmetry. Thus, it was reported that the electric dipoles of $\mathbf{1}_{\text{Por}}$ are in parallel and perpendicular orientations to the ethane bridge linking the two porphyrin macrocycles, while the directions of the corresponding transitions in $\mathbf{1}$ are polarized along the axes connecting the nitrogen atoms of the diametrically opposite pyrrole rings in a chlorin unit (see Figure 1).^{1a,3,9} This will lead to modulation of the coupling direction and rotatory (as well as oscillator) strength of the corresponding electronic transitions even if the geometry of these two bis-chromophoric systems is the same, thus controlling the overall supramolecular chirogenesis. For example, on the basis of the exciton chirality method¹² it can be easily predicted that the syn and fully extended anti conformation should be CD silent in bis-porphyrins due to the parallel orientation of the coupling transitions. However, in the case of bis-chlorins these conformations are optically active due to the perpendicular orientation of the degenerate coupling transitions (see Supporting Information).¹³ The third essential difference is a relative oscillator strength of the B- and Q-bands. It is well-known that, in general, porphyrin structures possess intense absorption in the region of the B-band, while the intensity of the Q transitions is negligibly small owing to its quasi-allowed character that makes it practically unusable for chirogenic purposes. Contrary to this, chlorines, besides their intense B absorption, exhibit reasonably large Q_y -bands that are polarized along the *y* axis (see Figure 1),¹⁴ hence offering greater advantages in studying the chirality issues because of its energetically isolated and well-defined spectral location. The fourth distinguishing fea-

(5) (a) Jordan, P.; Fromme, P.; Witt, H. T.; Klukas, O.; Saenger, W.; Krauss, N. *Nature* **2001**, *411*, 909. (b) Zouni, A.; Witt, H. T.; Kern, J.; Fromme, P.; Krauss, N.; Saenger, W.; Orth, P. *Nature* **2001**, *409*, 739. (c) McDermott, G.; Prince, S. M.; Freer, A. A.; Hawthornthwaite-Lawless, A. M.; Papiz, M. Z.; Cogdell, R. J.; Isaacs, N. W. *Nature* **1995**, *374*, 517. (d) Kühlbrandt, W.; Wang, D. N.; Fujiyoshi, Y. *Nature* **1994**, *367*, 614.

(6) (a) Zheng, G.; Shibata, M.; Dougherty, T. J.; Pandey, R. K. *J. Org. Chem.* **2000**, *65*, 543. (b) Jaquinod, L.; Senge, M. O.; Pandey, R. K.; Forsyth, T. P.; Smith, K. M. *Angew. Chem., Int. Ed. Engl.* **1996**, *35*, 1840. (c) Tamiaki, H.; Miyatake, T.; Tanikaga, R.; Holzwarth, A. R.; Schaffner, K. *Angew. Chem., Int. Ed. Engl.* **1996**, *35*, 772.

(7) Smith, K. M.; Bisset, G. M. F.; Bushell, M. *J. Bioorg. Chem.* **1980**, *9*, 1.

(8) Chernook, A. V.; Shulga, A. M.; Zenkevich, E. I.; Rempel, U.; von Borzyskowski, C. *J. Phys. Chem.* **1996**, *100*, 1918.

(9) For a preliminary account of the part of this work related to the enantiomer separation, spatial structure, and assignment of the absolute configuration of the corresponding bis-chlorin antipodes see: Borovkov, V. V.; Muranaka, A.; Hembury, G. A.; Origane, Y.; Ponomarev, G. V.; Kobayashi, N.; Inoue, Y. *Org. Lett.* **2005**, *7*, 1015.

(10) Smith, K. M. *Porphyrins and Metalloporphyrins*; Elsevier: Amsterdam, 1975.

(11) Senge, M. O.; Hope, H.; Smith, K. M. *J. Chem. Soc., Perkin Trans. 2* **1993**, 11.

(12) Harada, N.; Nakanishi, K. *Circular Dichroic Spectroscopy. Exciton Coupling in Organic Stereochemistry*; University Science Books: Mill Valley, CA, 1983.

(13) Using the example of the bis-porphyrin tweezer system, it was shown previously that only the degenerate couplings contribute significantly to the induced optical activity (see ref 3a).

(14) (a) Houssier, C.; Sauer, K. *J. Am. Chem. Soc.* **1970**, *92*, 779. (b) Gouterman, M. In *The Porphyrins, Volume III, Physical Chemistry, Part A*; Dolphin, D., Ed.; Academic Press: New York, 1978. (c) Keegan, J. D.; Stolzenberg, A. M.; Lu, Y.-C.; Linder, R. E.; Barth, G.; Moscovitz, A.; Bunnenberg, E.; Djerassi, C. *J. Am. Chem. Soc.* **1982**, *104*, 4305. (d) Keegan, J. D.; Stolzenberg, A. M.; Lu, Y.-C.; Linder, R. E.; Barth, G.; Moscovitz, A.; Bunnenberg, E.; Djerassi, C. *J. Am. Chem. Soc.* **1982**, *104*, 4317.

TABLE 1. UV–Vis and CD Spectral Data of **1** and the Resulting Supramolecular System **1**·**L** with Different Chiral and Achiral Amines^a

system	UV–vis data		CD data					
	$\lambda_{\max}(\text{nm})$ [$\epsilon/10^5(\text{M}^{-1} \text{cm}^{-1})$]		$\lambda_{\max}(\text{nm})$ [$\Delta\epsilon_n(\text{M}^{-1} \text{cm}^{-1})$]					
	B transition	Q transition	B transition		Q transition			
			1st Cotton ($n = 1$)	2nd Cotton ($n = 2$)	$ A ^b$	1st Cotton ($n = 1$)	2nd Cotton ($n = 2$)	$ A ^b$
1	406 [1.89], 414 [1.81]	622[0.67]			0			0
1 · 2_R	417 [2.14]	627 [0.63]	430 [+25.0]	415 [−9.5]	+34.5	640 [−16.5]	630 [+6.4]	−22.9
1 · 2_S	417 [2.15]	627 [0.63]	430 [−23.6]	417 [+11.0]	−34.6	638 [+12.1]	628 [−8.2]	+20.3
1 · 3_R	418 [2.18]	627 [0.64]	434 [+14.2]	422 [−8.3]	+22.5	642 [−4.9]	631 [+14.3]	−19.2
1 · 3_S	418 [2.16]	628 [0.64]	434 [−12.3]	424 [+6.2]	−18.5	643 [+3.9]	633 [−12.9]	+16.8
1 · 4_R	417 [2.13]	627 [0.64]	430 [−5.3]	415 [+4.2]	−9.5			0
1 · 4_S	417 [2.11]	627 [0.64]	429 [+4.9]	413 [−3.1]	+8.0			0
1 · 5_R	417 [2.17]	627 [0.64]	428 [−20.1]	417 [+11.0]	−31.1	638 [+8.3]	627 [−5.5]	+13.8
1 · 5_S	417 [2.14]	627 [0.63]	429 [+17.3]	418 [−9.4]	+26.7	640 [−5.1]	626 [+7.5]	−12.6
1 · 6_S	418 [2.08]	627 [0.63]	429 [+11.9]	419 [−10.5]	+22.4	642 [−5.1]	626 [+8.3]	−13.4
1 · 7_R	417 [2.03]	627 [0.64]	428 [−5.3]	417 [+7.2]	−12.5	637 [+5.1]	627 [−3.7]	+8.8
1 · 7_S	418 [2.03]	627 [0.64]	429 [+4.8]	418 [−4.8]	+9.6	640 [−4.2]	626 [+4.4]	−8.6
1 · 8_S	417 [2.10]	627 [0.64]			0			0
1 · 9_S	418 [2.19]	627 [0.64]	429 [+18.2]	419 [−10.7]	+28.9	637 [−9.8]	624 [+12.0]	−21.8
1 · 10_S	419 [2.18]	629 [0.65]	430 [+48.6]	419 [−29.3]	+77.9	639 [−31.6]	626 [+22.9]	−54.5
1 · 11_R	418 [2.13]	627 [0.63]	430 [−20.8]	418 [+6.2]	−27.0	643 [+11.2]	633 [−4.4]	+15.6
1 · 11_S	418 [2.18]	628 [0.64]	431 [+24.3]	419 [−4.0]	+28.3	643 [−12.8]	633 [+5.4]	−18.2
1_R	406 [1.89], 414 [1.81]	622[0.67]	415 [+92.0]	401 [−71.0]	+163.0	633 [−78.1]	618 [+57.0]	−135.1
1_R · 2_R	417 [2.14]	627 [0.63]	430 [+44.9]	414 [−24.2]	+69.1	638 [−37.3]	624 [+27.5]	−64.8
1_R · 2_S	417 [2.16]	627 [0.61]	433 [−6.2] ^c	422 [+5.6] ^c	−11.8 ^c	636 [−5.6]	620 [+15.9]	−21.5
1_S	406 [1.89], 414 [1.81]	622[0.67]	414 [−90.0]	402 [+72.0]	−162.0	633 [+77.9]	618 [−55.5]	+133.4
1_S · 12	417 [2.15]	627 [0.63]	429 [−50.8]	414 [+32.0]	−82.8	636 [+49.8]	622 [−30.2]	+80.0
1_S · 13	417 [2.17]	627 [0.63]	427 [−30.1]	412 [+25.6]	−55.7	637 [+29.1]	623 [−26.2]	+55.3

^a $C_1 = (3.2\text{--}4.5) \times 10^{-6} \text{ M}$, $C_L = 4.1 \times 10^{-2} - 1.4 \times 10^{-1} \text{ M}$ in CH_2Cl_2 . ^b $|A| = \Delta\epsilon_1 - \Delta\epsilon_2$. This value represents the total amplitude of the CD couplets. The CD recording accuracy based on the baseline evaluation is $\pm 3 \text{ M}^{-1} \text{ cm}^{-1}$. ^c There is a third relatively small Cotton effect at 413 nm ($-4.0 \text{ M}^{-1} \text{ cm}^{-1}$).

ture of the bis-chlorin structure is that **1** in contrast to **1_{Por}** is an intrinsically chiral compound with four stereogenic centers. Theoretically this may lead to the possible existence of a complex mixture of several enantiomeric, diastereomeric, and achiral (meso) forms. However, in practice, as shown by chiral HPLC analysis, the synthesized bis-chlorin product is a racemic mixture consisting of the two enantiomers **1_R** and **1_S** exclusively, in which all asymmetric carbons are of *R* or *S* absolute configurations, correspondingly.⁹

Amines have been chosen as external guests because of their well-known ability to coordinate to zinc complexes of tetrapyrrolic compounds and form stable pentacoordinate adducts at room temperature.¹⁰ To investigate the influence of different structural factors on supramolecular chirogenesis in the bis-chlorin, various commercially available amines **2–13**, shown in Figure 1, have been used as external ligands in this study. Particularly, chiral guests **2–11** being of the same structures as used in previous studies^{1a,3h,i} have been selected to adequately compare the role of the chlorin and porphyrin host structures on the chirogenic processes. Additionally, achiral guests **12** and **13** have been chosen to examine the modulation of chiroptical properties of the corresponding enantiopure bis-chlorin hosts upon complexation with external ligands.

Hence, to investigate interactions of the hosts **1** and **1_R/1_S** with the amine guests **2–13** in detail, several spectroscopic methods have been applied.

2. UV–Vis Spectral Properties. In the beginning, the complexation behaviors of **1** and **1_R/1_S** with **2–13** were examined by absorption spectroscopy.

All of the UV–vis spectra of the host–guest complexes **1(1_R/1_S)·L** exhibit essentially the same spectral pattern regardless of the ligand used, and are markedly different from those of the initial non-interacting **1(1_R/1_S)** (Figures 2–4, Table 1). These spectral changes are associated with the ligation process and subsequent conformational transformations of the bis-chlorins into the anti form (in the case of inside coordination⁴), and are additionally supported by ¹H NMR spectroscopy (see below). Thus, at amine-saturated concentrations, where the 1:2 host–guest complex is formed exclusively due to the pentacoordinate properties of zinc complexes of tetrapyrrolic macrocycles,¹⁵ the B transition profile is changed from the well-resolved split pattern (406 and 414 nm) into a single peaked band with the maximum at 417–419 nm having a small shoulder at ca. 402 nm, while Q-bands are bathochromically shifted up to 7 nm. Although these spectral changes clearly indicate amine coordination at the zinc chlorin moieties and consequent p_z - a_{2u} ligand–chromophore orbital mixing, as well as conformational changes induced by the host–guest interactions, they are less pronounced than those observed in the case of **1_{Por}**.^{1a,3h–m} However, this can be easily predicted upon consideration of the degree of interchromophoric electronic communication and spatial arrangement of the two

(15) The complex stoichiometry and binding mechanism have been previously comprehensively studied for the analogous bis-porphyrin systems (see ref 3h).

chlorin moieties in **1**, which strongly influences various spectroscopic properties (particularly, the positions of the absorption bands and chemical shifts). As discussed above, the initial conformation of ligand-free **1** resembles, to some extent, the tweezer conformation in **1_{Por}**, which is an intermediate state between the two terminal syn and anti forms. Since, as shown previously, moving from the tweezer conformation to the anti form is accompanied by only moderate UV–vis spectral changes (particularly, low-energy transition shifts) in comparison to the drastic transformations observed upon the syn–anti conformational switching,^{3c} one can expect that the respective spectral changes of **1** upon interaction with external guests should be also modest. However, it is likely that the observed UV–vis spectra are a result of summation of various conformational forms of the **1**(**1_R**/**1_S**)·**L** complexes as discussed below.

3. CD Spectral Properties. In contrast to the similar absorption properties, the optical activities of the bis-chlorin complexes studied are strongly affected by the ligand structure and by the host and guest chirality, thus dividing all supramolecular assemblies into three major categories: racemic host with chiral guests, chiral host with chiral guests, and chiral host with achiral guests.

3.1. Racemic Host with Chiral Guests. While the parent racemic **1** is as expected optically inactive, interaction with chiral amines results in remarkable CD behavior. Particularly, **1**·**L** shows variable optical activities in both the B and Q regions (Table 1, Figure 2) in sharp contrast to **1_{Por}**·**L**, which exhibits induction of the CD signal only in the B-band region.^{1a,3} This is due to the enhanced oscillator strength of the Q_y transitions of **1** as detailed above. The induced B and Q CD signals consist of two Cotton effects and are of opposite sign, indicating the different polarization of its major contributing electronic transitions along the chlorin *x* and *y* axes (see Figure 1). Specifically, since the low-energy couplet arises from coupling of the Q_y transitions, it is reasonable to assume that the major contribution to the high-energy couplet comes from the corresponding B_x transitions. Another distinguishing feature of the induced optical activity in **1**·**L** is the absence of a direct correlation between the guest's absolute configuration and the CD sign, which is also in contrast with the corresponding relationship established for **1_{Por}**·**L**.^{1a,3} For example, although the majority of (*S*)-amines (**4_S**–**7_S**, **9_S**–**11_S**) induce a positive CD couplet in the region of Soret band, as it is in the case of **1_{Por}**, there are two clear exceptions, **2_S** and **3_S**, which generate negative chirality. This apparent discrepancy produces the remarkable effect of chirality inversion upon increasing the ligand's bulkiness within the same homologous type, such as for **2**–**5**. The relative bulkiness of the ligands in Figure 1 has been addressed in previous work.^{1a,3i,1} Comparing the chirality-generating power of the corresponding guests in **1**·**L** and **1_{Por}**·**L**, it was found that the overall CD amplitudes (*A* values) of **1**·**L** are smaller than those of **1_{Por}**·**L** (the *A* values of **1_{Por}**·**L** have been reported previously³ⁱ). This decrease in the chirogenic sensitivity leads to the situation in which ligands having a weak chirogenic effect (in comparison to the analogous induced chirality in **1_{Por}**·**L** due to, for example, the remote chiral center position, such as for **8_S**) are unable to adequately transfer their asymmetry information to **1**, thus producing the CD silent complexes.

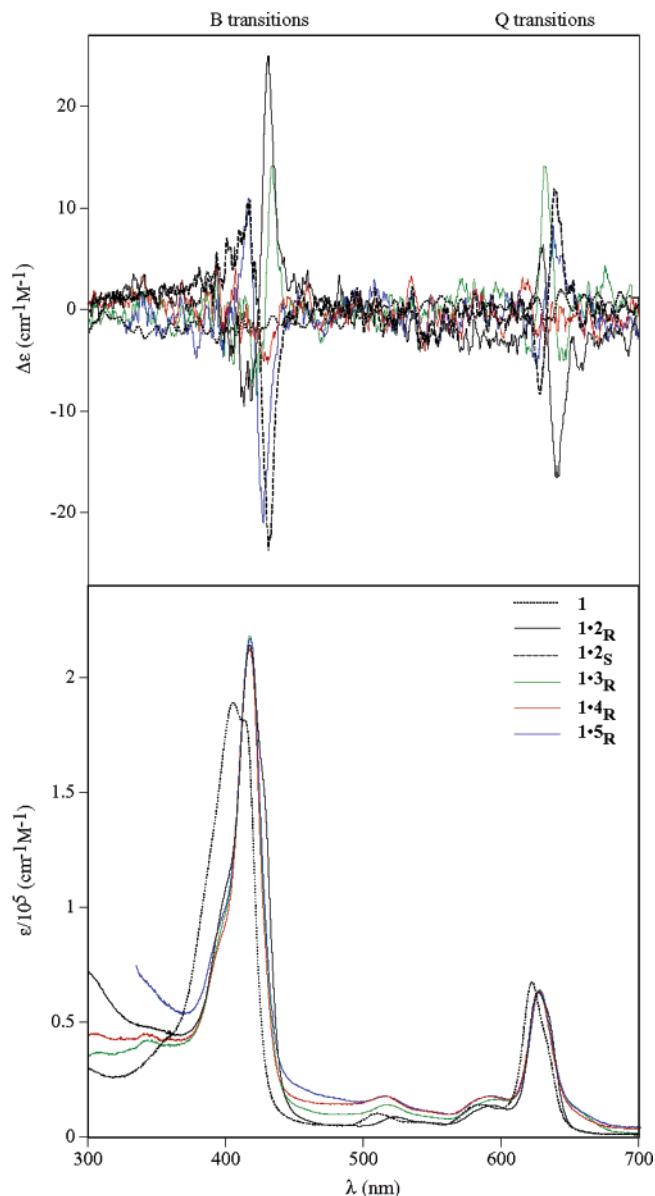


FIGURE 2. UV–vis (bottom) and CD (top) spectra of achiral **1** in CH₂Cl₂ at 295 K without ligand and in the presence of different chiral amines.

Apparently, this specific chirogenic behavior is associated with the structural and electronic peculiarities of **1**. However, to rationalize the mechanism of supramolecular chirogenesis in **1** upon interaction with chiral guests, two other classes of supramolecular assemblies (chiral host with chiral and with achiral guests) should be also investigated.

3.2. Chiral Host with Chiral and Achiral Guests. For the first class of supramolecular assemblies (chiral host and chiral guests) **1_R** was used as a chiral host, while **2_R** and **2_S** were selected as chiral guests owing their greatest chirogenic power among the other enantiomeric pairs, which have been tested for inducing chirality in racemic **1** (Table 1). Since **1_R** is inherently optically active, the through-space homocoupling of the B (corresponding to B_x and B_y) and Q (specifically Q_y) transitions results in the appearance of two strong couplets in the CD spectrum consisting of two Cotton effects (*A* values

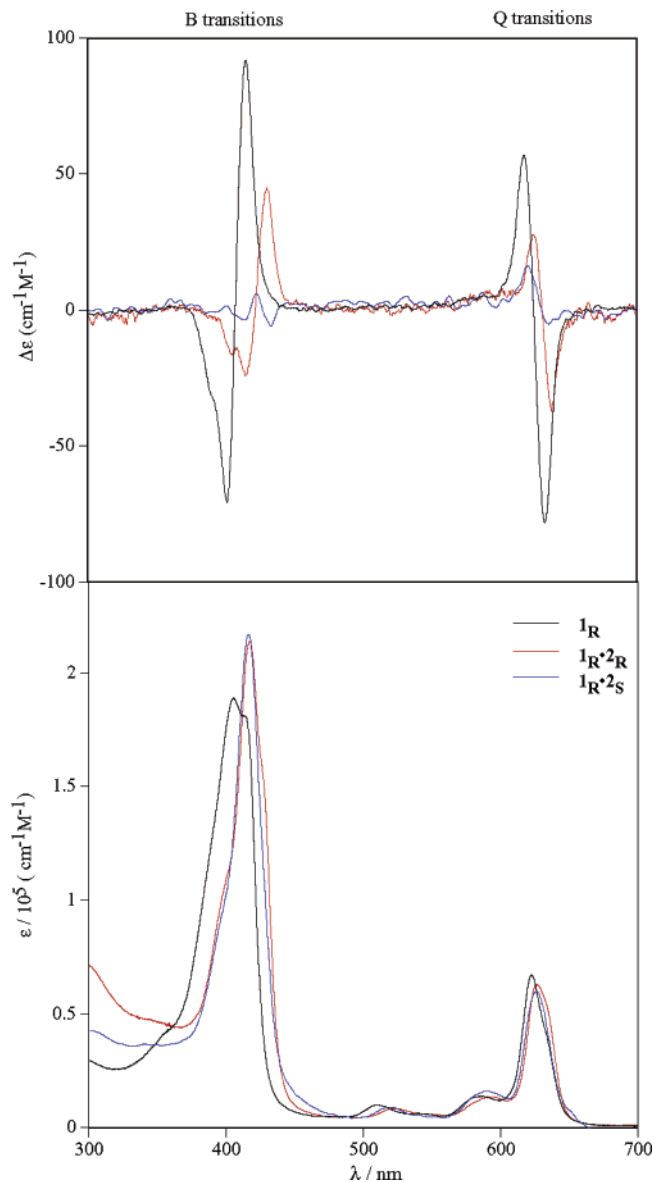


FIGURE 3. UV-vis (bottom) and CD (top) spectra of chiral $\mathbf{1}_R$ in CH_2Cl_2 at 295 K without ligand and in the presence of enantiomeric amines $\mathbf{2}_R$ and $\mathbf{2}_S$.

are $+163$ and $-135 \text{ cm}^{-1} \text{ M}^{-1}$, respectively). The detailed description and rationalization of the chiroptical properties of $\mathbf{1}_R$ have been reported previously.⁹ Upon the interaction of $\mathbf{1}_R$ with enantiopure $\mathbf{2}_R$ and $\mathbf{2}_S$ there are several significant changes in the CD spectra (Table 1, Figure 3). The first one is the bathochromic shifts of the corresponding CD signals along with similar low-energy shifts of the UV-vis absorption bands, which arise from formation of the pentacoordinate complexes as in the case of the $\mathbf{1}\cdot\mathbf{L}$ systems. The second feature is a considerable reduction of the A values of $\mathbf{1}_R\cdot\mathbf{2}_R$ and $\mathbf{1}_R\cdot\mathbf{2}_S$ in comparison to that of the original $\mathbf{1}_R$, indicating that some of the supramolecular complexes formed possess opposite chirality that decreases the CD intensity. The third feature, which is the most important, is a clear difference in the resulting CD spectral profiles upon interaction with antipodal guests. For example, in the region of the Q_y transitions the CD couplet of $\mathbf{1}_R\cdot\mathbf{2}_S$ is 3 times smaller than that of $\mathbf{1}_R\cdot\mathbf{2}_R$, while in the case of the B transitions

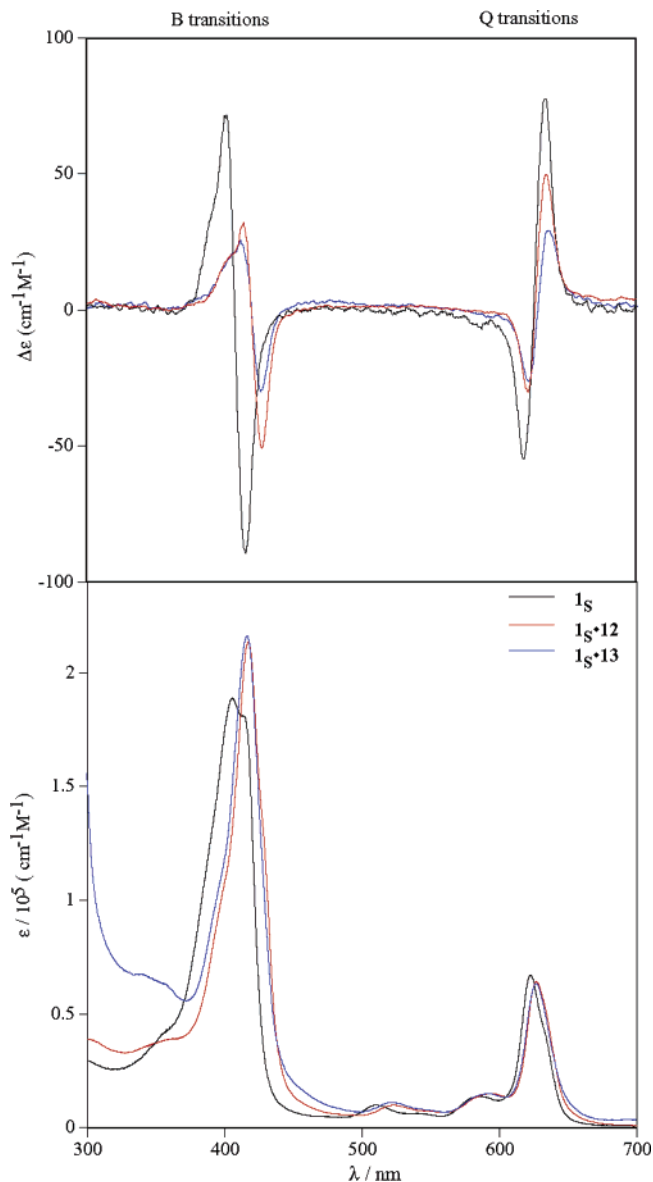


FIGURE 4. UV-vis (bottom) and CD (top) spectra of chiral $\mathbf{1}_S$ in CH_2Cl_2 at 295 K without ligand and in the presence of achiral amines $\mathbf{12}$ and $\mathbf{13}$.

the first Cotton effect of $\mathbf{1}_R\cdot\mathbf{2}_S$ is even inverted. This pronounced differentiation alludes to the distinct spatial arrangement of these diastereomeric complexes, which can be applied for chiral recognition purposes.¹⁶

For the second type of supramolecular assemblies (chiral host and achiral guests) antipodal $\mathbf{1}_S$ was used as a chiral host, while $\mathbf{12}$ and $\mathbf{13}$ were selected as achiral guests as they are of the same structural homologous type and distinguished by the substituent size. As expected, the CD spectrum of $\mathbf{1}_S$ is a perfect mirror image of $\mathbf{1}_R$ (Figure 4). The effects of the interaction of $\mathbf{1}_S$ with $\mathbf{12}$ and $\mathbf{13}$ are similar to those observed for chiral guests $\mathbf{2}_R$ and $\mathbf{2}_S$, which include bathochromic shifts of the corresponding CD signals and noticeable reduction of the A values (Table 1, Figure 4). Additionally, a marked decrease of the CD amplitude upon increasing ligand

(16) This study is currently in progress and will be reported in due course.

bulkiness is observed (in the case of the Q_y transitions: +80 versus +55 $\text{cm}^{-1} \text{M}^{-1}$ for $1_S \cdot 12$ and $1_S \cdot 13$, correspondingly), thus indicating geometrical differences between these complexes.

It can be inferred then that the above-described absorption and CD spectral changes are a result of certain conformation changes in the bis-chlorin hosts upon interaction with external ligands. By analogy with the corresponding bis-porphyrins, it is reasonable to suggest that the complexation process is a complex multistep equilibrium with several species of different geometries. To shed light on this problem, ^1H NMR spectra were taken at the various host–guest molar ratios.

4. ^1H NMR Spectral Properties. The ^1H NMR spectrum of ligand-free **1** reflects well the structural peculiarities and geometry of the bis-chlorin host (see Supporting Information). Particularly, all the meso and ethane bridge protons are well-resolved, while the methylene protons of the Et substituents form several complex multiplets ($\delta = 4.5\text{--}2.5$ ppm), which are expected considering the structural asymmetry of the chlorin macrocycle. The tweezer type of spatial organization of **1**^{9,11} shows that only the protons of the Et group at the *c* position locate closely enough to the neighboring chlorin ring to be appreciably affected by its ring-current effect, while other protons are too distant. Therefore, this situation predicts a strong upfield shift of the corresponding proton resonances in relation to their usual position, a situation which can indeed be seen in the respective ^1H NMR spectrum (-0.41 and -1.60 ppm for the CH_2 and CH_3 protons, respectively). Although in the case of **1**, in contrast to **1_{Por}**, there are no specific interchromophoric interactions that can be broken by the complexation process (thus inducing the prominent syn–anti conformational changes found previously in the bis-porphyrin systems), the external ligation may induce certain conformational changes, particularly upon inside coordination. If this is the case, then primarily the protons exposed to the ring-current effect should be most affected. As one can see, upon the stepwise addition of chiral ligands **2_R** and **4_R** to **1** the ^1H NMR spectral profile of bis-chlorin part is essentially unchanged, with the exception of the $-\text{C}(\text{c})\text{CH}_2\text{CH}_3$ protons' resonances which undergo profoundly large downfield shifts ($\Delta\delta$); for example, the $\Delta\delta$ values of $-\text{C}(\text{c})\text{CH}_2\text{CH}_3$ are 0.8 and 0.41 ppm for **1**·**2_R** and **1**·**4_R**, respectively.¹⁷ These transformations clearly indicate that a conformational switching takes place and the corresponding anti species, which are responsible for the chirality induction in **1**, are likely to be formed along with other conformational species.

Additionally, since **1** is a racemic mixture, interaction with an enantiopure guest should yield two diastereomeric complexes **1_R·L** and **1_S·L** (also as a mixture of various spatial conformers) which are distinguishable by ^1H NMR spectroscopy. Indeed, this effect is clearly observed in the case of **1**·**2_R**, which exhibits a noticeable split of the corresponding meso protons into two singlets of equal intensities at high host:guest ratios (see Supporting Information).

(17) The less pronounced shift of **1**·**4_R** is apparently caused by a compensation effect of the ligand's aromatic substituent.

5. Mechanism of Supramolecular Chirality Induction and Modulation. 5.1. Racemic Host with Chiral Guests. Although, in general, the spectral changes observed in **1** upon interaction with chiral guests allude to the host–guest association and subsequent chirogenic processes occurring in **1_{Por}**, the specific structural and electronic features of the bis-chlorin host, which result in several distinct differences in the corresponding optical activities, should be properly taken into consideration. Particularly, the initial tweezer-type geometry of **1**^{9,11} dictates that the first external ligand may relatively easily approach either of the two central zinc ions of the bis-chlorin from both the inside and outside manners. This is in sharp contrast to the exclusively outside first ligation occurring in **1_{Por}** because of its folded syn conformation. Also, due to the absence of strong inter-chlorin interactions in **1** (the breaking of which in **1_{Por}** accounts for the subsequent syn–anti conformational switching), the “outside coordination” does not induce such drastic conformational changes, thus largely preserving the initial tweezer-type arrangement of the chlorin moieties. However, contrarily the inside coordination of a guest should generate specific steric repulsive interactions with the ethyl groups of the neighboring chlorin moiety, so yielding the extended anti form as in the case of **1_{Por}**, and that was indeed found by monitoring the ^1H NMR spectroscopy. This variability already predicts the existence of at least two conformers of the corresponding monoligated species: the tweezer type (similar to the initial form) upon outside coordination and the anti form upon inside coordination. In the same manner, the direction of the second ligation occurring in the neighboring chlorin ring can also be from both sides, which may affect the overall geometry of supramolecular system as well. In short, these multi-variant possibilities should result in a complex mixture of the host–guest assemblies possessing different geometries. However, as was also previously stated for **1_{Por}**,^{1a,3} only the inside coordination is paramount for supramolecular chirogenesis owing to the competitive steric repulsion between the substituents at the stereogenic center of chiral guest and the *a*- and *b*-ethyl groups of the neighboring porphyrin ring, while the outside coordination gives only negligible or no chirality induction. Therefore, in the case of **1** it is also expected that upon the outside coordination there are no appreciable specific chirality-inducing interactions, which are able to break enantiomeric parity of the corresponding racemic mixture and, thus, produce noticeable CD signals. Furthermore, neither outside nor inside guests' binding to **1** can facilitate rotation around the $-\text{C}(\text{meso})-\text{CH}_2-$ bond of the ethane bridge,¹⁸ which may also generate an enantiomeric excess. Hence, the only plausible rationalization of the induced optical activity in **1**·**L** is a conformational difference between the corresponding diastereomeric anti complexes of **1_R·L** and **1_S·L**, where **L** is the corresponding enantiomerically pure guest of the *R* or *S* absolute configuration.

(18) On the basis of crystallographic structure and CPK model examinations of the corresponding *trans*-ethylene-bridged and *anti*-ethane-bridged bis-porphyrin analogues (see Kitagawa, R.; Kai, Y.; Ponomarev, G.; Sugiura, K.-i.; Borovkov, V.; Kaneda, T.; Sakata, Y. *Chem. Lett.* **1993**, 1071. Hitchcock, P. B. *J. Chem. Soc., Dalton Trans.* **1983**, 2127.) it was concluded that the steric hindrance imposed by the *a*-, *b*-ethyl groups of the two chlorin moieties makes the rotation around the $-\text{C}(\text{meso})-\text{CH}_2-$ bonds of the ethyl bridge impossible.

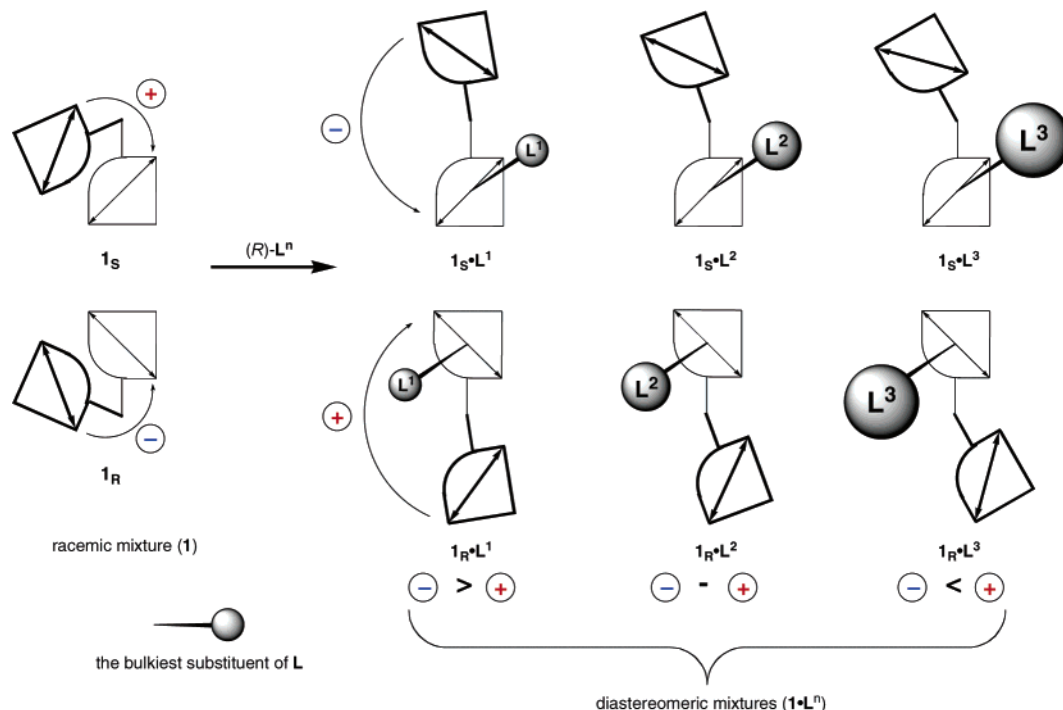


FIGURE 5. Schematic representation of the supramolecular chirality induction in racemic **1** upon interaction with chiral amines of different bulkiness (R)- L^n .

Although quantitative analysis of the chirogenic events in **1** is a far too difficult task for current methods, due to the above-mentioned complexity of the multistep association process and the large number of the equilibrium species, qualitatively the mechanism of chirality induction can be depicted in Figure 5. Taking into account the discussed driving forces of supramolecular chirogenesis, and for the sake of simplicity, only the anti products of inside coordination are shown, with only the interactions between the bulkiest substituent of a chiral amine and the neighboring chlorin ring considered. For additional clarity, only the coupling of the electronic transitions polarized along the y axes are presented and discussed, while the effect of the x transitions' interaction can be easily understood, considering their perpendicular orientation (see Figure 1). Particularly, the choice of the y transition as the diagnostic tool is dictated by its energetic separation in the Q-band region which allows unambiguous rationalization of the obtained spectral data, without interference from the second degenerate coupling. As an example, the interaction of **1** with (R)-ligands, (R)- L^n , of different bulkiness ($n = 1-3$, see Figure 5) is demonstrated, while the interaction with (S)-ligands should give the exact mirror image structures. Thus, inside binding of (R)- L^n to **1** yields two diastereomers $1_R \cdot L^n$ and $1_S \cdot L^n$. In the case of conventional monodentate ligands, in which the substituent size order correlates with the Cahn–Ingold–Prelog priority rule for absolute configuration assignment, it is apparent that the bulkiest substituent at the stereogenic center of L^n interacts with the a -ethyl group of 1_S and with the b -ethyl group in the case of 1_R , so forcing the two chlorin moieties to form left-handed screws in both diastereomeric complexes. This mechanism of helicity induction in **1** is generally the same as that in 1_{Por} .^{1a,3} However, unlike 1_{Por} , the electronic transitions in **1** are polarized distinctly

along the direction of the pyrrole rings (see Figures 1 and 5). This results in the situation that the y transitions in 1_S and 1_R (as well as the x transitions) are orientated opposite to each other. Therefore, the same left-handed screws in $1_R \cdot L$ and $1_S \cdot L$ give different directions of through-space degenerate coupling for the corresponding electric dipoles:¹³ anticlockwise for $1_S \cdot L$ and clockwise for $1_R \cdot L$. These, according to the exciton chirality method,¹² correspond to negative and positive chirality. Thus, if the energy levels and rotational strengths of the induced CD couplets in both diastereomeric complexes are equal, they should compensate for each other, resulting in a CD silent spectrum, however this is clearly not the case. The rationale for the observed optical activity resides in the different spatial arrangements of the coupling transitions in $1_S \cdot L$ and $1_R \cdot L$. For example, one can easily notice that the angles between the pairs of y coupling transitions in $1_S \cdot L^1$ (anticlockwise orientated) and in $1_R \cdot L^1$ (clockwise orientated) are significantly different, less and more than 90° , respectively, even if the dihedral angles between the two chlorin moieties are the same for both diastereomeric complexes.¹⁹ Although reliable theoretical treatment of the optical activity in the bis-chlorin-based supramolecular complexes is not available yet due to the complexity of these multicomponent systems, numerical calculations of the CD spectra of simple dibenzoates and related chromophores using the exciton chirality method¹² showed that the amplitude of Cotton effects has a parabolic-like dependence on the dihedral angle between the coupling transitions, with zero values at 0° and 180° and a maximum value at around 70° , see Figure 6. Assuming

(19) Indeed, the dihedral angle between the two chlorin moieties is dependent upon the degree of the steric repulsion between the bulkiest substituent of a chiral ligand and the a - and b -ethyl groups and may not be the same for $1_S \cdot L$ and $1_R \cdot L$, if these interactions are nonequivalent for the a - and b -ethyl groups.

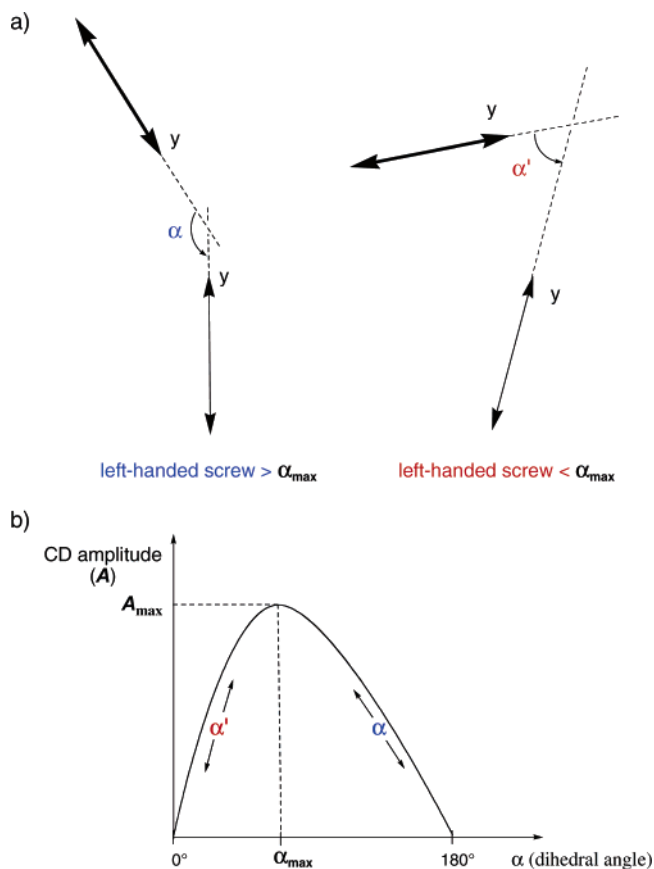


FIGURE 6. Electronic transitions (a), and schematic representation of the CD amplitude dependence on the dihedral angle (α) between the corresponding electronic transitions (b).

that, in general, the coupling electric dipoles follow this tendency, it is clear that the angle between the coupling y transitions in $\mathbf{1}_S\cdot\mathbf{L}^1$ is smaller than 90° (an exact 90° angle is found in the “no screw” fully extended anti conformation with the dihedral angle between two chlorin moieties at 180° , see Supporting Information) and closer to the optimal coupling, while in the case of $\mathbf{1}_R\cdot\mathbf{L}^1$ the corresponding angle is larger than 90° , thus reducing the amplitude of induced couplet. Hence, summation of the stronger negative couplet of $\mathbf{1}_S\cdot\mathbf{L}^1$ and weaker positive couplet of $\mathbf{1}_R\cdot\mathbf{L}^1$ results in a negative CD signal of moderate-to-small intensity, which is actually observed for the less bulky guests **2** and **3** (see Table 1 and Figure 2). However, this plausible rationalization cannot be used as a universal rule explaining the observed chirogenic processes in **1**. For example, the more bulky ligands **4** and **5** of the same homologous type, as well as other bulky guests **6**, **7**, and **9–11**, which are of different homologous types, exhibit a remarkable phenomenon of the chirality switching that requires further insight into the mechanism of supramolecular chirality induction.

5.2. Bulkiness Effect and Supramolecular Chirality Switching. The dramatic ligand size effect upon interaction with **1**, leading to the remarkable phenomenon of chirality switching, can be explained in terms of the above-mentioned A value’s dependence upon the variable angle between the corresponding coupling tran-

sitions (Figure 6). As one can see, further increasing the ligand bulkiness (see the \mathbf{L}^2 and \mathbf{L}^3 cases) results in enhancement of the degree of screw sense between the two chlorin moieties in both $\mathbf{1}_S\cdot\mathbf{L}$ and in $\mathbf{1}_R\cdot\mathbf{L}$, which in turn changes the angles between the coupling electric dipoles, i.e., the angle between the y transitions is decreased in the order $\mathbf{1}_S\cdot\mathbf{L}^1 > \mathbf{1}_S\cdot\mathbf{L}^2 > \mathbf{1}_S\cdot\mathbf{L}^3$ (see Figure 5), while the tendency is the opposite in the case of other diastereomeric complexes of $\mathbf{1}_R\cdot\mathbf{L}^n$. However, the exciton chirality method predicts that the ascending branch of the parabolic-like dependence of the A value upon the dihedral angle between the coupling transitions (from 0° to the maximum) is much steeper than that of the descending branch (from the maximum to 180°) (Figure 6).¹² This means that for the interacting y transitions in $\mathbf{1}_S\cdot\mathbf{L}$, the amplitude of the negative CD couplet decreases faster than the amplitude of the corresponding positive CD couplet. Therefore, it is reasonable to assume that this difference in the reduction of A values should result in the following situations: initially negative chirality dominates (\mathbf{L}^1), then these two couplets will begin to compensate each other, ultimately yielding a CD silent complex at a certain ligand size (\mathbf{L}^2), and finally the positive couplet will dominate over the negative one, thus switching the induced chirality sign upon further increasing the ligand bulkiness (\mathbf{L}^3). Indeed, such tendency is clearly seen for the homologous guests **2–5**; upon increasing the ligand size the negative Q_y couplet induced by (R)-amines is decreased (from **2_R** to **3_R**), almost quenched (for **4_R**), and finally becomes positive (for **5_R**) (see Table 1 and Figure 2). Moreover, other bulky enantiopure ligands (**6**, **7**, **9–11**) also exhibit the same behavior. In the case of (S)-amines the corresponding negative chirality is obtained with the greatest A value being $-54.5 \text{ M}^{-1} \text{ cm}^{-1}$ induced by the bulkiest ligand **10_S**.

Another distinctive property of the bis-chlorin host **1** is found to be a nonlinear-type dependence of the A value upon the effective size of homologous amines²⁰ (see Figure 7), which is in sharp contrast to the clear linear relationships observed for the bis-porphyrin host **1_{Por}**.^{31j} This difference appears to arise from the non-equivalence in the steric interactions between the bulkiest substituent of the chiral guest and the ethyl groups at the a - and b -positions of the neighboring chlorin ring (the pyrrole and the reduced pyrrole rings, respectively), and is an additional factor controlling the degree of screw sense in the diastereomeric complexes $\mathbf{1}_S\cdot\mathbf{L}$ and $\mathbf{1}_R\cdot\mathbf{L}$. This results in different dihedral angles between the chlorin moieties of $\mathbf{1}_S\cdot\mathbf{L}$ and $\mathbf{1}_R\cdot\mathbf{L}$, and, in turn, affects the linearity of the previously reported A value/effective size relationship found for **1_{Por}**.

As a result of the above-discussed chirality compensation effect, the sensoric properties of **1** are noticeably decreased in comparison with **1_{Por}**, as can be judged by the overall decrease of the induced CD signals and the inability to sense a remote chiral center (for example, at a β position to the amine binding group of **8_S**).

5.3. Chiral Host with Chiral Guests. As additional support to the discussed mechanism of chirality induction and switching in **1**, supramolecular interactions between the optically active host **1_R** and two antipodal guests are analyzed. As stated above, inside coordination yields the

(20) For definition of the effective size, see ref 3i.

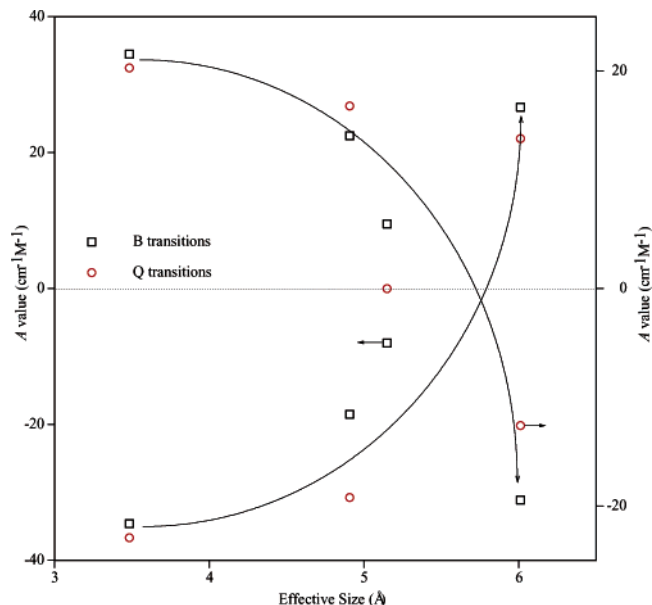


FIGURE 7. Dependence of the induced CD amplitude of **1** (*A* value) on the effective size of the amines.

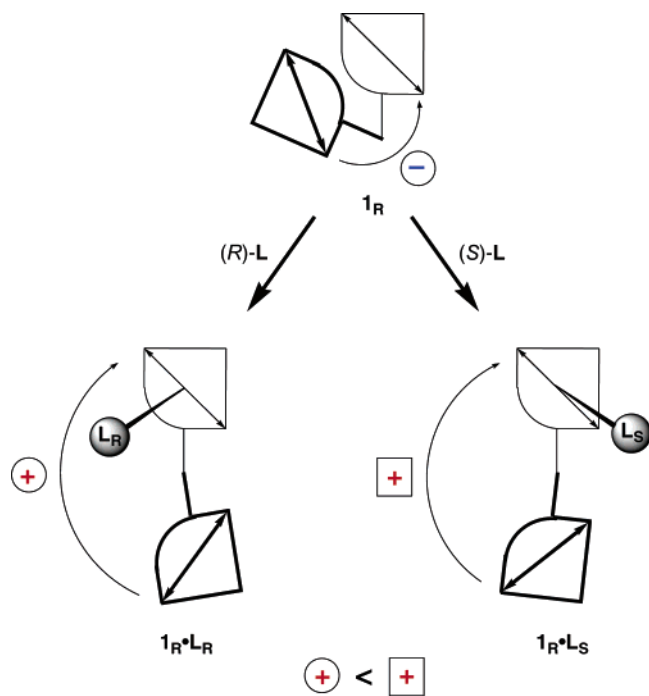


FIGURE 8. Schematic representation of the supramolecular chirality modulation in chiral **1_R** upon interaction with enantiomeric amines (*R*)-**L** and (*S*)-**L**.

corresponding anti complexes of inverted helicity, thus inducing opposite chirality. In the case of enantiomeric **1_R** this mode of ligation of *R* and *S* amines results in two anti diastereomeric complexes **1_R·L_R** and **1_R·L_S**, respectively (see Figure 8). It is clearly seen that, while the right-handed screw in **1_R** gives an anticlockwise orientation of the *Q_y* dipoles, thus leading to a negative CD couplet, the right- and left-handed screws in **1_R·L_S** and **1_R·L_R**, respectively, produce clockwise orientation of these transitions, thus inducing positive CD couplets in both diastereomeric complexes. However, the dihedral angles

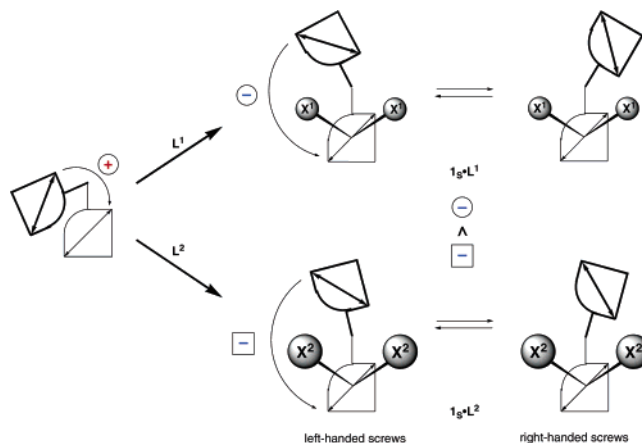


FIGURE 9. Schematic representation of the supramolecular chirality modulation in chiral **1_S** upon interaction with achiral amines **Lⁿ**.

between the corresponding transitions are apparently different: $<90^\circ$ for **1_R·L_S** and $>90^\circ$ for **1_R·L_R**. This, according to the exciton chirality method,¹² also anticipates induction of a positive CD couplet of higher intensity in the case of **1_R·L_S**. Taking into account that the resulting CD signal in **1_R·L** is a summation of the induced couplets with opposite signs generated by numerous conformations of different geometries, which depend on the mode of ligand approach as discussed above, one can expect the appearance of stronger positive chirality for **1_R·L_S** in comparison to **1_R·L_R**. This will be the case if the contribution of the outside coordination (which preserves the original screw handedness of the bis-chlorin) is relatively small; or alternatively, if the outside coordination is sufficient, the generation of the less-intense negative couplet is expected. Indeed the latter situation is realized, and consequently the *A* value of the *Q_y* couplet of **1_R** is decreased by 6.3 times upon interaction with **2_S**, but by just 2.1 times in the case of **2_R** (see Table 1 and Figure 3).

Hence, these data demonstrate clearly that the outside coordination in the **1·L** systems contributes sufficiently to control the chirality sign in the case of chiral hosts **1_R** and **1_S** owing to the opposite helicity of the “inside” (arising from the steric interactions) and “outside” (arising for the inherent chirality of **1_S** and **1_R**) coordinative complexes (although in the case of the racemic host **1** the outside coordination has only a minor or no effect on the induced chirality due to the compensation effect of the racemic mixture of corresponding left- and right-handed diastereomeric forms) and more importantly that the induced chirality is strongly affected by the geometry and particularly the coupling electric dipole orientation of the supramolecular systems.

5.4. Chiral Host with Achiral Guests. Further corroborative evidence for the proposed mechanism of supramolecular chirogenesis in **1** comes from interactions between the chiral host **1_S** and the achiral guests **12** and **13** of different bulkiness. By analogy with the above-discussed cases, the inside coordination also leads to the corresponding anti complexes of different screw senses but possessing the opposite chirality of the initial unbound or “outside binding” states (see Figure 9), resulting in an overall decrease in the CD amplitude (see Table 1

and Figure 4). However, in contrast to chiral amines, the relative size of two largest substituents at the carbon located at the α -position with respect to the amino binding site is the same, thus generating the equally probable right- and left-handed screw anti complexes possessing the same dihedral angle between the chlorin moieties.²¹ In both screw structures of $1_S \cdot L$ the Q_y transitions are coupled in an anticlockwise manner that corresponds to negative chirality, although the corresponding angles between these transitions are different: $<90^\circ$ for the left-handed screw and $>90^\circ$ for the right-handed screw. Therefore, the resulting negative chirality is a summation of these two forms.

Upon increasing the substituent size from X^1 to X^2 it is apparent that the two bulkier X^2 groups (for example, in the case of **13**) produce stronger steric repulsions with the ethyl groups of the neighboring chlorin ring, thus restricting its rotation around the ethane bridge, and consequently yield lesser screws in both the right- and left-handed anti conformations in order to minimize these steric hindrances (Figure 9). It is also obvious that the change of the degree of inter-chlorin screw effects the spatial orientation of the interacting chlorin transitions. For example, the dihedral angle between the Q_y dipoles of $1_S \cdot L^2$ becomes closer to 90° , hence enhancing the induced negative couplet, which in turn should further decrease the positive chirality induced upon outside ligation as in the above-discussed cases. Actually, this effect is clearly observed by the example of A value reduction for bulkier $1_S \cdot 13$ in comparison to less bulky $1_S \cdot 12$.

Conclusions

This work clearly demonstrates that, besides the external guest, the host's structure (including chemical, geometrical, and electronic) plays an important role in supramolecular chirogenesis by controlling the corresponding steric and electronic interactions. In particular, induced chirality is strongly dependent upon the coupling electronic dipoles' orientation and relative composition of the resulting supramolecular complexes, especially in the case of generation of opposite helicity. We see here the first example of the rationalization of the chirogenic

(21) Some deviations from the equal probability and dihedral angle are possible due to the different degree of the steric interactions between the ligand's bulkiest substituents and the ethyl groups of the neighboring chlorin moiety at the a and b -positions.

phenomena for the naturally occurring chlorin chromophores, at a level of conformational and chiral complexity previously inaccessible. This is a result of a detailed understanding and consideration of its electronic transitions and dynamics (along with influencing factors) and its judicious comparison with the well-studied porphyrin-based analogue. Thus, these results offer a clearer view of the chirality processes in natural and artificial assemblies, with the insights gained having the potential for practical implications in the design of chiroptical molecular devices. Specifically, an intensive low-energy absorption, possessing a high degree of anisotropy (in the case of chiral bis-chlorins), well-defined differences in the optical activity of the corresponding diastereomeric complexes, and a thorough understanding of the chirogenesis mechanism, makes it possible to apply these properties for chiral recognition purposes. These studies are currently in progress and will be the subject of future reports from our group.

Experimental Section

Materials. The racemic ethane-bridged host **1** was synthesized according to the previously reported methods^{2h,7} and compared with the reference spectral data.⁸ The enantiopure 1_R and 1_S were obtained by enantiomeric separation of **1** using preparative HPLC (eluent, MeOH at 35°C ; flow rate, 5.5 mL/min; UV detected at 380 nm), and the obtained fractions were analyzed by analytical HPLC (4.6×150 mm; eluent, MeOH at 35°C ; flow rate, 0.3 mL/min; UV detected at 370 nm). Chiral and achiral amines (see Figure 1), anhydrous CH_2Cl_2 for UV-vis and CD measurements, and CDCl_3 for ^1H NMR studies were purchased from commercial suppliers and used as received.

Spectroscopic Measurements. CD scanning conditions were as follows: scanning rate = 50 nm/min, bandwidth = 1 nm, response time = 0.5 s, accumulations = 1 scan. The saturated amine concentrations used for the UV-vis and CD measurements were the concentrations where the spectral changes associated with the chlorin chromophores were at their maximum, and further increase of the amine concentration had no effect on the signal intensities (for the amine and chlorine concentration ranges, see footnote *a* in Table 1).

^1H NMR spectra were recorded at room temperature ($C_1 = 1.9 \times 10^{-3}$ M, concentration of amines was changed from 0 to 9.5×10^{-3} M). Chemical shifts were referenced to the residual proton resonance in CDCl_3 (δ 7.25 ppm).

Supporting Information Available: Orientation of electronic transition coupling upon the bis-chlorin geometry and ^1H NMR spectra. This material is available free of charge via the Internet at <http://pubs.acs.org>.

JO051067D